Natural Hazards **4**: 171–191, 1991.

Numerical Simulation of Tsunamis – Its Present and Near Future

N. SHUTO
Department of Civil Engineering, Tohoku University, Aoba, Sendai 980, Japan

(Received: 15 March 1990; revised: 9 July 1990)

Abstract. Hindcasting of a tsunami by numerical simulations is a process of lengthy and complicated deductions, knowing only the final results such as run-up heights and tide records, both of which are possibly biased due to an insufficient number of records and due to hydraulic and mechanical limitation of tide gauges. There are many sources of error. The initial profile, determined with seismic data, can even be different from the actual tsunami profile. The numerical scheme introduces errors. Nonlinearity near and on land requires an appropriate selection of equations. Taking these facts into account, it should be noted that numerical simulations produce satisfactory information for practical use, because the final error is usually within 15% as far as the maximum run-up height is concerned.

The state-of-the-art of tsunami numerical simulations is critically summarized from generation to run-up. Problems in the near future are also stated. Fruitful application of computer graphics is suggested.

Key words. Tsunami initial profile, tsunami propagation, tsunami run-up, tsunami numerical simulation, tsunami secondary disaster, computer graphics.

1. Introduction

Numerical simulation has made much progress during the past 30 years and is now used as one of the most effective means in the practical design of tsunami defense works and structures. This progress was supported by the development of seismology and by the appearance of the high-speed computer. Seismology made it possible to estimate the fault mechanism and the related displacement of the sea bottom. This gives the initial profile of a tsunami which has never been measured on site with conventional methods of measurement. A huge near-field tsunami such as the 1933 Showa Great Sanriku tsunami has an extension, one to two hundred kilometers long and several tens of kilometers wide, when it is generated. The coast to be affected is several hundred kilometers long. If the effect of a distant tsunami such as the 1960 Chilean tsunami is discussed, the whole Pacific Ocean should be covered by a net of computation grids. This situation is only solved with electronic computers which ensure a huge computer memory and high-speed computation. A numerical simulation, if designed without due consideration, cannot provide any reliable results. There are many sources of error and misjudgement. If well-designed, its results can be used in practical tsunami defense works with sufficient accuracy, within 15% error as far as the maximum run-up heights and the

inundated areas are concerned. The aim of the present paper is to provide a critical review of the state-of-the-art of numerical simulation, to summarize problems which require further study in the near future, and to show utility of a new technique in understanding computed tsunamis.

In Section 2, the generation problem is examined, taking the 1983 Nihonkai-Chubu (the Middle Japan Sea) earthquake tsunami as an example. Contradictions are found among tsunami sources determined from seismic data, tide records, and run-up heights. Limitation of tide gauges is also discussed.

In Section 3, the propagation problem is discussed, mainly as the problem of fundamental equations and difference schemes. It is evident that a set of equations of higher-order approximation yield better results, if used with fine spatial grids. An ingenious method is introduced to obtain equivalent results with equations of first-order approximation and with rough spatial grids, thus saving much of the CPU time and computer money.

Section 4 reviews the near-shore and run-up problem, in which the major factors we encounter are the nonlinearity of the phenomena, instability in the computation, and approximation of the moving land boundary.

In Section 5, three topics are briefed for future study. A theory must be developed for edge bores which were observed in 1983. In relation to secondary disasters, spread of oils as well as spread and impact of floating materials are in urgent need of study. Computer-graphics-aided animation is promising as a way to understand tsunamis through computed results.

2. Generation of Tsunamis

2.1. *Three Source Models of the 1983 Nihonkai-Chubu Earthquake Tsunami*

At noon on the 26 May 1983, a huge earthquake occurred in the Japan Sea. A tsunami followed. Its highest run-up was measured at more than 15 m above the mean sea-water level. Several features of the tsunami were made clear by tide records, detailed surveys of run-up height and inundated areas, and many photos and videos.

As for the earthquake, more scientific means were available. For example, positions of the major shocks and every after-shock were three-dimensionally determined as in Figure 1 (Takagi *et al.*, 1984). An immediate conclusion is that the fault dips slightly eastward. Fault mechanism and fault parameters were determined from seismic data collected not only locally but also world-widely.

Figure 2(a) shows the vertical displacement of the sea bottom, calculated by Tanaka *et al.* (1984) with the Mansinha and Smylie (1971) method. Since the source was large compared with the water depth and the rupture velocity was very short compared with the tsunami propagation velocity, the bottom vertical displacement gave the vertical displacement of the free water surface, i.e. the initial tsunami profile. Only seismic data were used in this calculation. The major result is that a

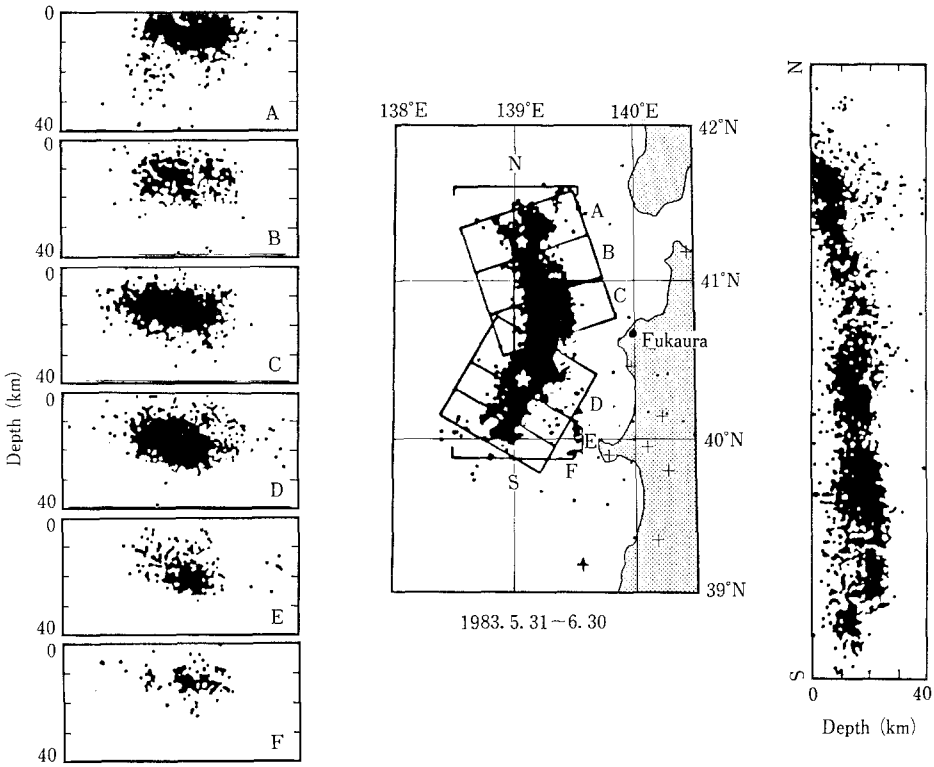

Fig. 1. After-shocks of the 1983 Nihonkai-Chubu earthquake.

maximum vertical displacement of about 1.5 m high is obtained at the western side of the source, corresponding to the fault which dips eastward. Tanaka *et al.* verified the computed displacement by comparison with the measured displacement at Kyuroku Island.

Figure 2(b) is the result obtained by Satake (1985). He used the tide records at 13 tide stations to modify the bottom displacement obtained from seismic data. The method of modification will be briefed in Section 2.3. According to his results, the fault dips eastward and the maximum vertical displacement is about 2 m.

Figure 2(c) is the result of a thorough study by Aida (1984a). The fault dips eastward and the maximum vertical displacement is about 4 m. He needed this maximum vertical displacement in order to explain run-up heights. He used seismic data, tide records at remote tide stations, and run-up data on the coast near the source. Based upon his rich experience, Aida did not use tide records at tide stations near the source, because he might be led to an incorrect conclusion by the fact that the hydraulic characteristics of a tide well often render it unable to record high frequency components of a nearby tsunami. He used run-up data in a way described in Section 2.3. His conclusion was verified by the present author who used

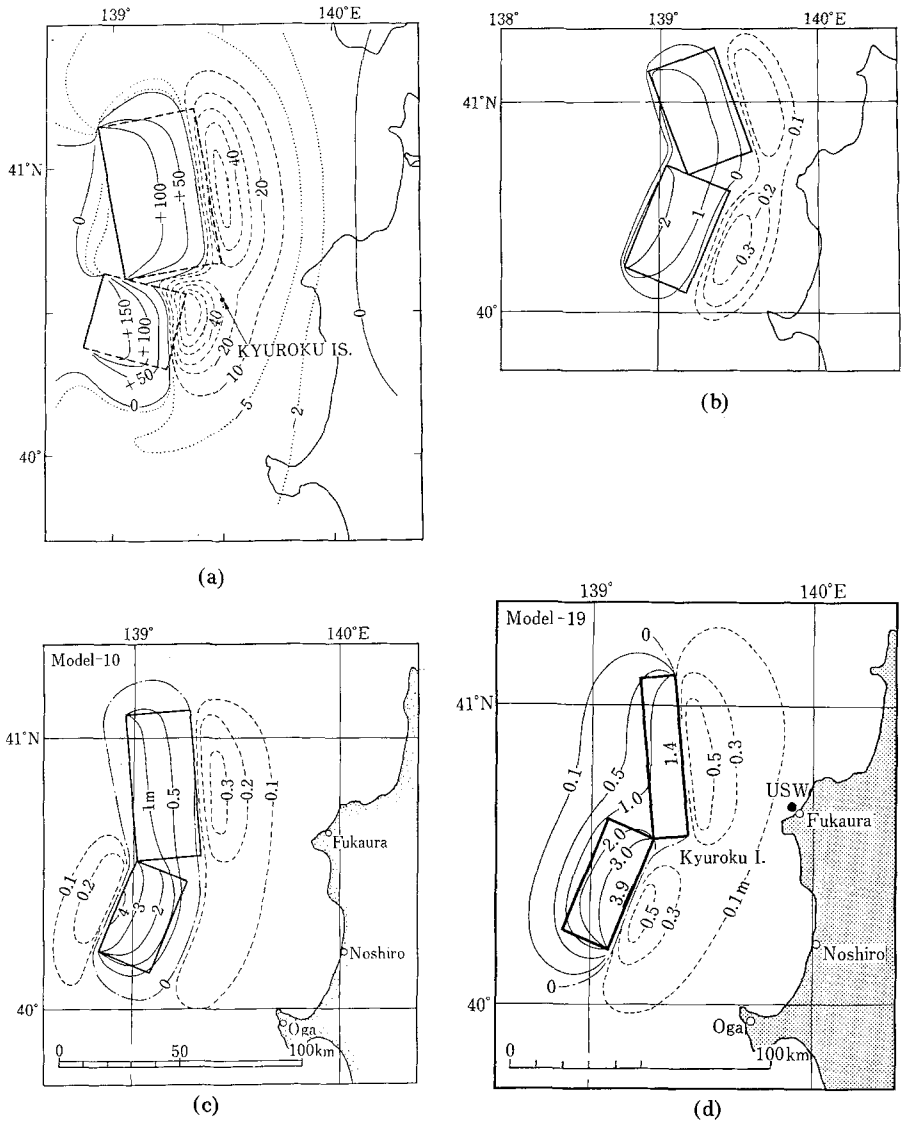

Fig. 2. Vertical displacement of sea bottom due to the 1983 Nihonkai-Chubu earthquake. (a) Tanaka *et al.*, (b) Satake Model D2, (c) Aida Model No. 10, and (d) Aida Model No. 19.

a finer grid length than usual and obtained the maximum run-up height of 15 m. The results has been published elsewhere (Shuto *et al.*, 1986).

2.2. *Aida Model No. 19, a Contradiction*

An ordinary tide gauge has three problems in recording tsunamis: hydraulic filtering, poor resolution with respect to time, and possible saturation in the case of a huge tsunami. A tide well is usually constructed to eliminate high-frequency

sea-level fluctuation, such as wind waves and swells. This characteristic also deteriorates the tsunami recording ability of a tide gauge. Satake *et al.* (1988) measured the hydraulic filtering characteristics of 40 tide wells and corrected tsunami records of the 1983 Nihonkai-Chubu earthquake tsunami. They found that some tide records should be more than doubled in amplitude.

This results, and the poor temporal resolution, suggest that we should be very careful when we compare the computed tsunami profiles with tide records for verification of the initial tsunami profile. Knowing this fact well, Aida tried another effort to estimate the initial profile of the 1983 tsunami. It was fortunate for him that a supersonic wave gauge for measuring wind waves and swells was available. This instrument recorded the initial small fall and the succeeding sharp rise of the 1983 tsunami, although the signal was superposed by short wind waves. This wave gauge measured directly the vertical distance to the water surface without any filtering. The temporal resolution was excellent, because the wave gauge should measure wind waves of only several seconds long.

Aida thought this record gave the most reliable tsunami profile. He struggled again and again to reproduce this tsunami profile by numerical simulation and arrived at a surprising conclusion – the Aida Model No. 19, shown in Fig. 2(d) (Aida, 1984b). It required that the fault should dip westward, contradicting seismic knowledge, although the maximum vertical displacement of the sea bottom was about 4 m, the same as his Model No. 10.

A possible explanation to mediate the contradiction may be the existence of a secondary fault, as in the case of the 1964 Great Alaska earthquake, as shown in Figure 3 (Plafker, 1965).

In conclusion, the present method, based upon seismic data, can be applied to establish the initial tsunami profile to a first-order approximation, but it does not give a full explanation of the tsunami. In hindcasting, correction should be made by using measured data: tide records and run-up heights. In forecasting, there are no alternatives.

2.3. *Verification in Terms of Aida's K and κ*

In order to examine whether the assumed initial tsunami profile is satisfactory or not, Aida (1978) introduced two measures, K and κ. In his original paper, he compared the first rise or fall of computed profiles with measured tide records, with no regard to the succeeding waves which were much affected by local topographical effects. The measure K is a geometric mean of the ratio of the measured amplitude to the computed, and κ is the corresponding standard deviation. If K is smaller than unity, it means the assumed tsunami initial profile (or the assumed total tsunami energy) is larger than the true solution. Therefore, he could multiply the assumed initial vertical displacement by the obtained value of K to obtain a reduced estimate. Another measure κ shows whether or not distribution of the vertical displacement is appropriate.

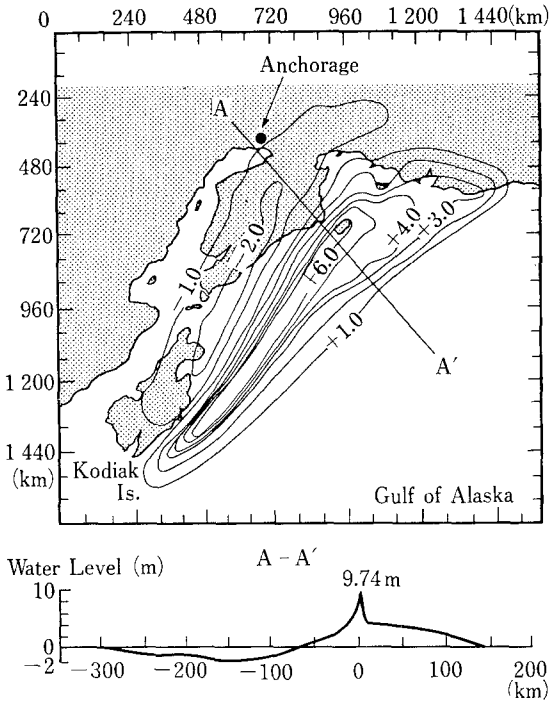

Fig. 3. Vertical displacement of ground and sea bottom of the 1964 Great Alaska earthquake.

Since the number of tide records available is usually 10 or so, not many for a tsunami, and since no tide record was available for a tsunami in the remote past, Aida extended the above method to apply to run-up heights, too. Measured run-up heights might strongly reflect local topography effects. He divided the coastal line into segments 10 or 15 km long. After smoothing the measured data by taking the average over each segment, he compared these smoothed values with the computed results obtained along the water depth contour of 200 m. If the ratios of the former to the latter are between 2 and 3 (= average run-up ratio), and if the value of κ is within an appropriate range, he judged that the assumed initial profile gave the solution.

With the initial profile thus given, a detailed numerical simulation can be carried out, including the reproduction of local topography effects. For the final judgement of whether or not the simulation gives satisfactory run-up heights, the same method is applied with no processing of the measured and computed data. For practical purposes, a numerical simulation is judged to be satisfactorily carried out if K falls between 1.2 and 0.8 and κ is less than 1.4 after necessary modification of the initial profile. Then, for a well-designed simulation, the final error is within 15% as far as the maximum run-up height is concerned (e.g., Aida and Hatori, 1984; Hasegawa, 1986; Shuto *et al.*, 1987).

3. Propagation in Deep Sea

3.1. *Linear Longwave Theory and Grid Length for No Decay*

At the time of generation, a tsunami in the water several kilometers deep is several tens of kilometers wide and up to 100 km long. Its height is less than 10 m. The depth-to-length ratio is on the order of 10^{-2} and the wave steepness is of order 10^{-3}. These values suggest that the linear longwave theory is a good first-order approximation.

Numerical simulations provide only approximate solutions, with errors inevitably included in and dependent on numerical techniques. In the following discussions, the leap-frog scheme is assumed for discretizing fundamental differential equations.

Figure 4 shows examples of computed wave profiles. Taking a sectional profile of the 1964 Great Alaska earthquake tsunami measured along the A–A line in Figure 3 as the initial profile, the one-dimensional propagation on water of constant depth is computed with the linear longwave theory. This theory gives a unique wave celerity which is not influenced by phase and amplitude dispersion effects. The true solution, therefore, should give the mere translocation without any change in the wave profile. It is evident, however, from the figures, that the wave profile deforms, depending upon the spatial grid length and the travel distance. The smaller the grid length is and the shorter the travel distance is, the truer the solution becomes. The change is that the leading wave reduces its height and a small wave-train appears behind it.

In order to eliminate this kind of numerical decay in wave height, the grid length should be carefully determined. According to numerical experiments by Shuto *et al.* (1986), one local tsunami wavelength should be covered by more than 20 grid points. Thus, the decay is less than 5% after the wave travels over a distance of four wavelengths, which is the longest travel distance for the first wave in the case of a typical near-field tsunami near the Japanese Archipelago. This condition should be satisfied, not only in deep oceans, but also in shallow seas.

3.2. *Dispersion Effect and Equations*

It was Kajiura (1963) who introduced a criterion to determine whether or not the dispersion effect should be taken into consideration. If his P_a defined by

$$P_a = (6h/R)^{1/3}(a/h) \tag{1}$$

is smaller than 4, the dispersion effect is not negligible. Here, h is the water depth, R is the travel distance, and a is the length of the tsunami source measured along the direction of propagation.

When the dispersion term is required, we have to switch from the linear longwave theory to the Boussinesq or linear Boussinesq equations. Under the same conditions as in Figure 4, the one-dimensional propagation is computed with the three equations: linear long wave, linear Boussinesq, and Boussinesq equations for two

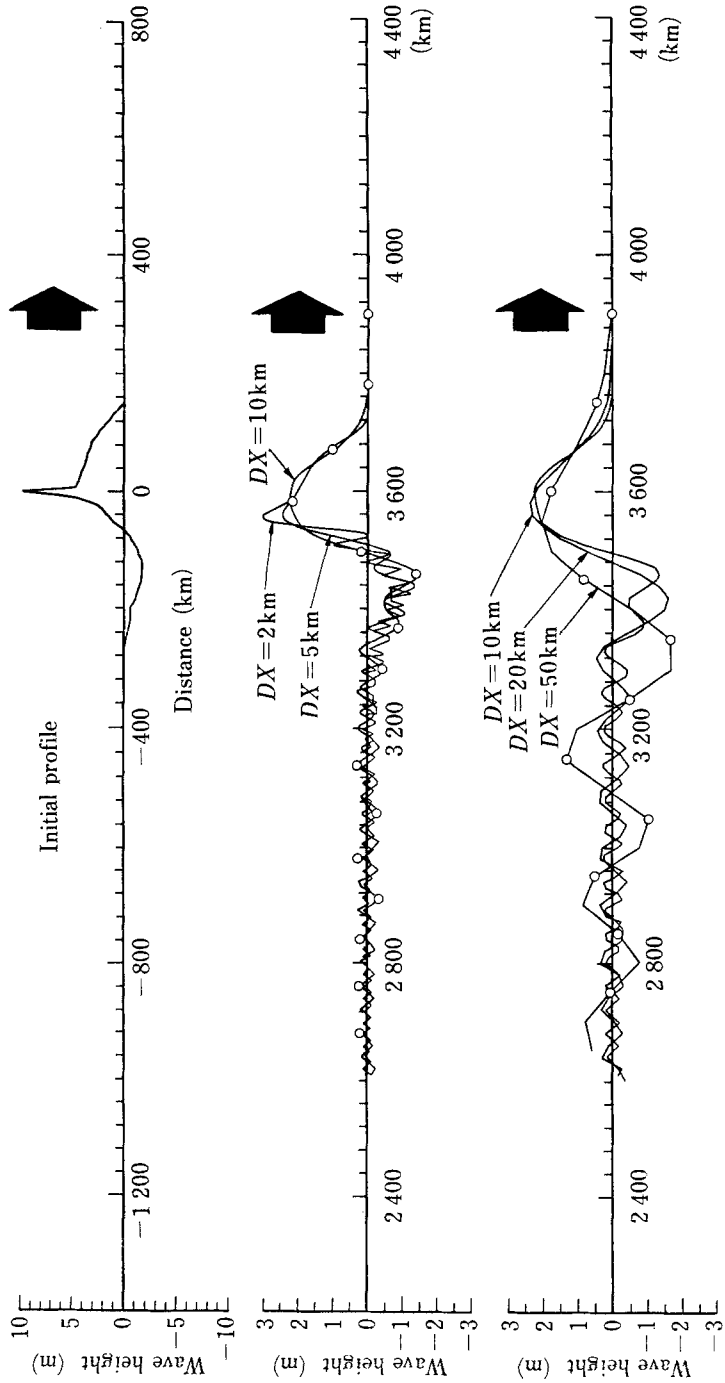

Fig. 4. Numerical results with the linear longwave theory for different grid length.

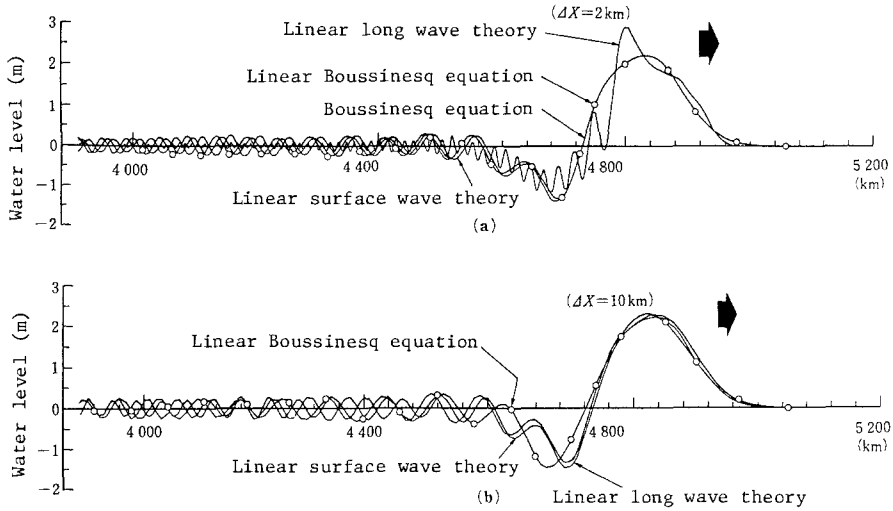

Fig. 5. Comparison of three longwave theories. The true solution is given by the linear surfacewave theory. (a) $\Delta x = 2$ km, and (b) $\Delta x = 10$ km.

different grid lengths. Figures 5(a) and 5(b) compare the results with the results of the linear surfacewave equation. By using the theory of linear surface waves, which fully includes the dispersion effect, the true solution is obtained as follows. The initial profile is decomposed into the Fourier components, which are translated with their own celerity. Then, the component waves are summed up to reconstruct the wave profile.

With the fine grid, the linear Boussinesq and Boussinesq equations almost coincide with the true solution, suggesting that the nonlinear term is not important in the propagation of a tsunami in deep ocean. The linear longwave theory deviates from the true solution in spite of the fine grid length.

On the other hand, with the coarse grid, the linear Boussinesq equation gives a satisfactory result for the major wave but a poor agreeement for the oscillation behind the major wave. This means that a higher-order equation with a fine grid gives better results. On the contrary, it is interesting to notice that the linear longwave equation with the coarse grid yields a better result. It is better than a higher-order equation with the same grid length and also better than itself with the fine grid length. This is due to the numerical dispersion.

3.3. *Numerical Dispersion and Its Use*

When a differential equation is reduced to a difference equation, approximation errors are inevitably introduced. The property and magnitude of the errors depend on the type of original equation and discretization scheme. In the following discussion, the staggered leap-frog scheme is used.

Equation (2) for the linear long waves,

$$\frac{\partial \eta}{\partial t}+\frac{\partial M}{\partial x}=0, \qquad \frac{\partial M}{\partial t}+C_0^2\frac{\partial \eta}{\partial x}=0 \tag{2}$$

is reduced to the following difference equation

$$\begin{aligned}&\eta_{i+1/2}^{n+1/2}-\eta_{i+1/2}^{n-1/2}+\frac{\Delta t}{\Delta x}[M_{i+1}^n-M_i^n]=0,\\ &M_i^{n+1}-M_i^n+C_0^2\frac{\Delta t}{\Delta x}[\eta_{i+1/2}^{n+1/2}-\eta_{i-1/2}^{n+1/2}]=0.\end{aligned} \tag{3}$$

Here, η is the water surface elevation, M is the discharge per unit width, C_0 is the celerity of linear long waves, x and t are the space and time coordinates, Δx and Δt are their grid lengths, the superscript n is the time grid number, and the subscript i is the spatial grid number.

Equation (3) is an approximation of Equation (2). In reverse, if Equation (3) is regarded as the true equation, Equation (2) is an approximation having errors. On making corrections to include the first term of the errors, a better differential expression of Equation (3) than Equation (2) is given as follows

$$\frac{\partial^2 \eta}{\partial t^2}-C_0^2\frac{\partial^2 \eta}{\partial x^2}-\frac{C_0^2\Delta x^2}{12}(1-k^2)\frac{\partial^4 \eta}{\partial x^4}=0, \tag{4}$$

in which k is the Courant number defined by $k=C_0\Delta t/\Delta x$. The third term is the numerical dispersion. Although it is of the order of the square of the grid length, the accumulated effect becomes nonnegligible after a long travel.

The linear Boussinesq equation, a higher-order longwave equation which has the physically required dispersion term, is given by

$$\frac{\partial^2 \eta}{\partial t^2}-C_0^2\frac{\partial^2 \eta}{\partial x^2}-\frac{C_0^2h^2}{2}\frac{\partial^4 \eta}{\partial x^4}=0, \tag{5}$$

in which h is the water depth.

It is Imamura (1989) who proposed the use of numerical dispersion in place of physical dispersion, by setting equal the coefficients of the third terms in Equation (4) and (5). When the grid length is selected so that the following Imamura number is nearly equal to unity

$$I_m=\Delta x[1-(C_0\Delta t/\Delta x)^2]^{1/2}/2h, \tag{6}$$

the linear longwave equation gives the same results as the linear Boussinesq equation, thereby saving much of the CPU time and computer memory.

Since the dispersion effect is not a strong effect, it is not necessary to make the Imamura number strictly equal to unity. Figure 5(b), in which the Imamura number is 1.4, shows a good agreement between the true solution and the result of the linear longwave theory.

3.4. *Coriolis Force*

In a simulation of a tsunami traveling the Pacific Ocean, the Coriolis force is necessarily included. However, in the 'ray method' often used to forecast the arrival time of a tsunami, no Coriolis force is taken into consideration. Figures 6(a) and 6(b) compare the contours of the highest water level in the Pacific Ocean computed for the 1969 Chilean tsunami with and without the Coriolis force. Due to the Coriolis force, the divergence and the convergence of the tsunami, i.e. its height as a result, are different, but the arrival time shows no large difference.

4. Near-Shore and Run-Up Problems

4.1. *Nonlinearity and Equations*

Entering shallow water and approaching the shore, a tsunami increases in height, steepness, and curvature of water surface. Equations change according to the order of approximation required to describe it: the linear longwave theory, the shallow-water theory, the Peregrine equation (1967) and the Goto equation (1984).

In seas deeper than 50 m, the linear longwave theory gives satisfactory results. As water depth decreases, the equations should be switched to the shallow-water theory with bottom friction. Generally speaking, the shallow-water theory is believed sufficient in tsunami simulation as far as the maximum run-up height and inundated area are concerned. It is, however, not sufficient in regard to the estimated wave force, which is closely related to wave profiles.

Figure 7 compares two higher-order equations with hydraulic experiments. The Peregrine equation shows an early dispersion which accelerates the fission of waves and leads to an increase in height. Although the Goto equation gives better results in this example, the range of its application has not yet been examined. In addition, if a higher-order equation is extended to the two-dimensional problem, the computation becomes extremely complicated. No attempt has been made to carry out a two-dimensional tsunami simulation with equations higher than the shallow-water theory.

4.2. *Examples of Instability*

4.2.1. *Instability near the Side Boundary.* When the capacity of a computer is not large enough compared with the number of grid points and the time required for a full computation, it is a usual technique to divide the computation into two stages, the offshore computation and the near-shore computation.

In the offshore computation, the entire region, from the tsunami source area to the land boundary, is covered with a net of coarse grids 3 and 5 km long for a near-field tsunami and about 10 km long for a far-field tsunami. The offshore computation assumes perfect reflection from the shoreline, the shape of which is

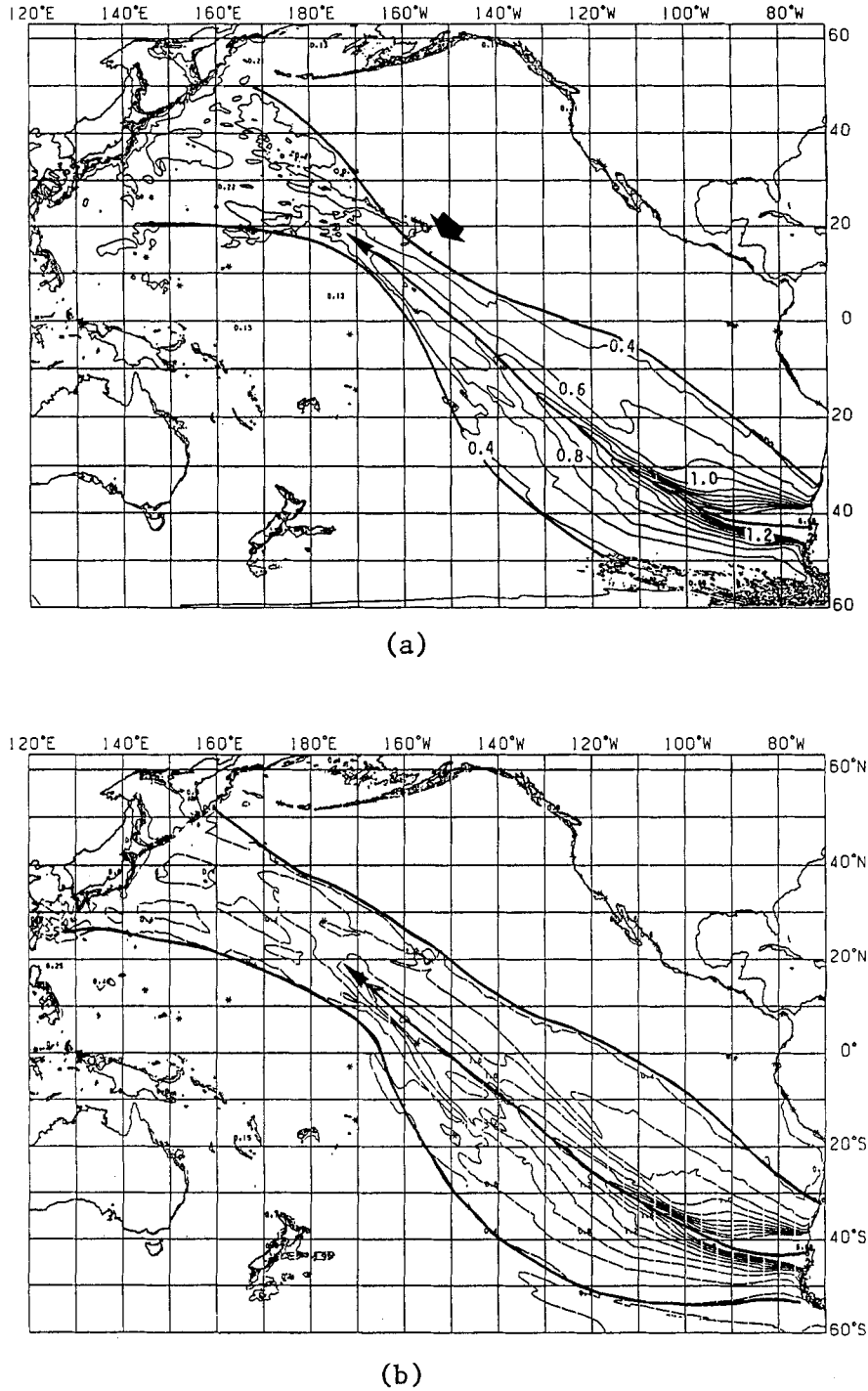

Fig. 6. Computed highest water level of the 1960 Chilean tsunami (a) with and (b) without the Coriolis force.

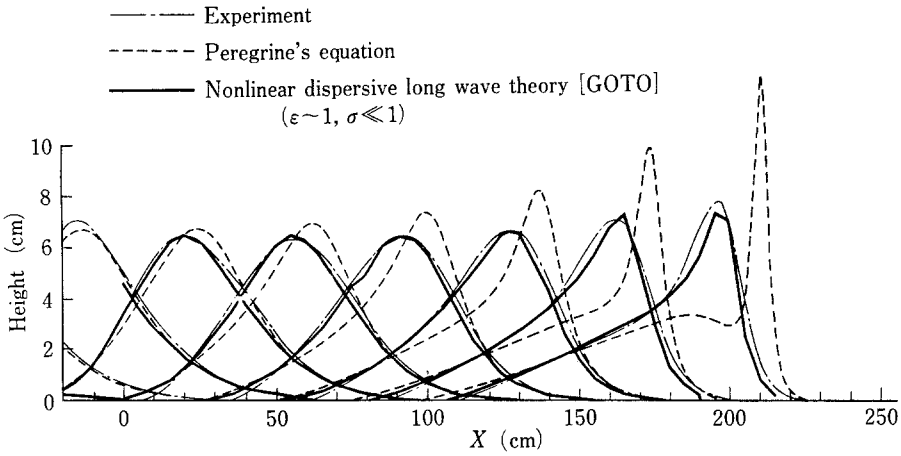

Fig. 7. Computed results with the Peregrine and Goto equations compared with hydraulic experiment.

very roughly approximated. Computed results, therefore, reflect effects of topography on a large scale. In other words, the results are only reliable at points in deep sea far from the land boundary, where effects of run-up and small-scale topography become unimportant.

The next stage is the near-shore computation, in which a net of fine grids varying from 1 km in deep sea to several tens of meters on land is used to allow observation of more limited areas, including areas of special concern. The area in the nearshore computation is enclosed by four boundaries: the land boundary, the open-sea boundary (which is usually set in the neighborhood of 1000 m contour and nearly parallel to the land boundary), and two side boundaries normal to the open-sea boundary. When outputs of the offshore computation at the coarser grid points are inputted on the open-sea and side boundaries in the near-shore computation, linear interpolations are used to determine the input at the finer grid points interposed between the coarser grid points. These interpolated values are only approximations, not the true solution, which will be obtained with the near-shore computation. Before waves reflected from land arrive at the boundaries, no difference between the assumed and true boundary values give serious influence to the computation. Even when reflected waves arrive at the far boundaries in deep sea, no serious discrepancy is found between the assumed input and the results of the detailed near-shore computation, because wave components reflecting effects of small-scale topography rapidly die out. On the contrary, in the shallow sea, in particular in the neighborhood of a corner where the major shoreline and the side boundary intersects with an acute angle, the reflection immediately arrives at the side boundary and often gives a considerable difference between the interpolated values and the computed results. This is the cause of an instability which will propagate rapidly and demolish the whole computation. Figure 8 shows an example of this kind of instability.

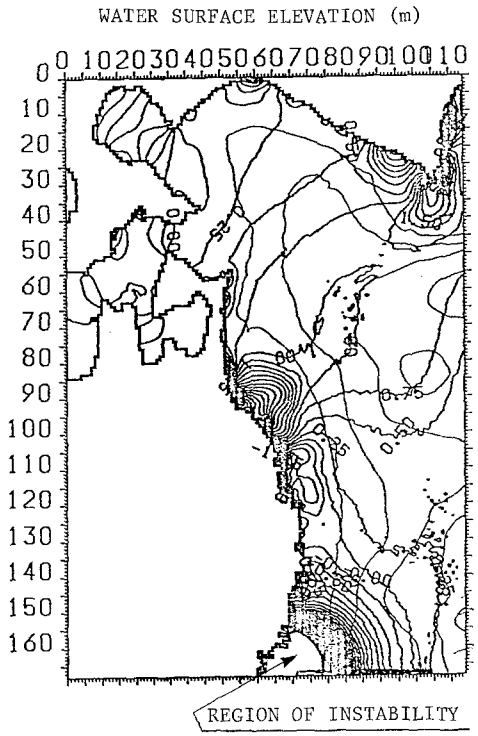

Fig. 8. Initiation of an instability at a corner of the boundary.

4.2.2. *Instability at the Front.* Figures 9(a) and 9(b) show examples of another instability. This oscillation occurs at the front of the second wave, which is running up against the back wash of the first wave. The second wave is retarded, its front surface steepens, and the oscillation occurs. With a smaller grid length, the length of instability waves is shorter. Evidently, this is a numerical instability dependent on the grid length used.

A method to eliminate this instability was introduced by Goto and Shuto (1983a). They use an artificial diffusion which acts to cancel the instability waves only in the vicinity of the wave front. When the artificial diffusion acts well, the front surface becomes more gently sloping than the front should be. An artificial viscosity is used to amend this over-smoothing, at the expense of negligible dissipation of energy. Figure 9(c) is an example of this method.

4.3. *Moving Boundary Approximation*

A tsunami front runs up and down the land. It is not easy to express this moving boundary with the coordinate system in the Eulerian description. If equations in the Lagrangian description are used, the moving boundary condition can be expressed

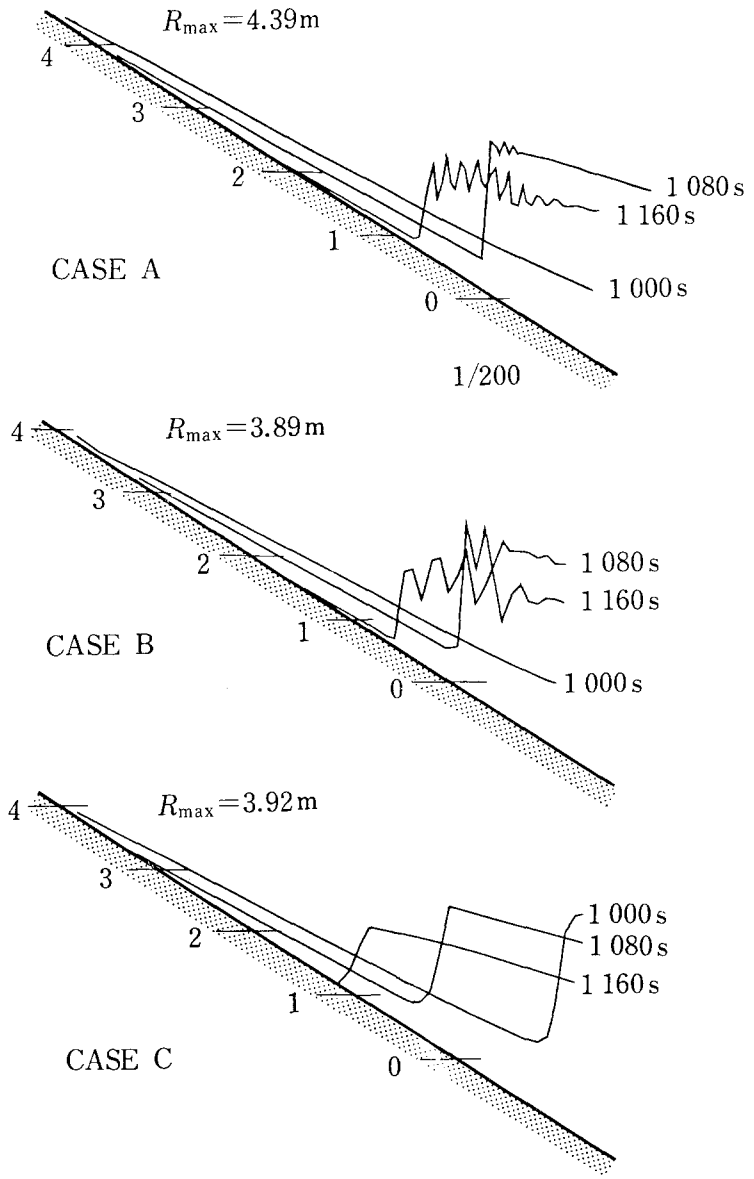

Fig. 9. Oscillation induced at the wave front (a) with $\Delta x = 12.5$ m and (b) with $\Delta x = 25$ m. (c) Wave profiles without oscillations obtained using the artificial diffusion term.

with no approximation (Shuto and Goto, 1978). Even with equations in the Eulerian description, a variable transformation in which the origin of the new coordinates is located at the front can easily express the moving boundary (Takeda, 1984). It is unfortunate, however, that these two methods are well applicable only to one-dimensional problems, but poorly to any two-dimensional practical problem with complicated topography.

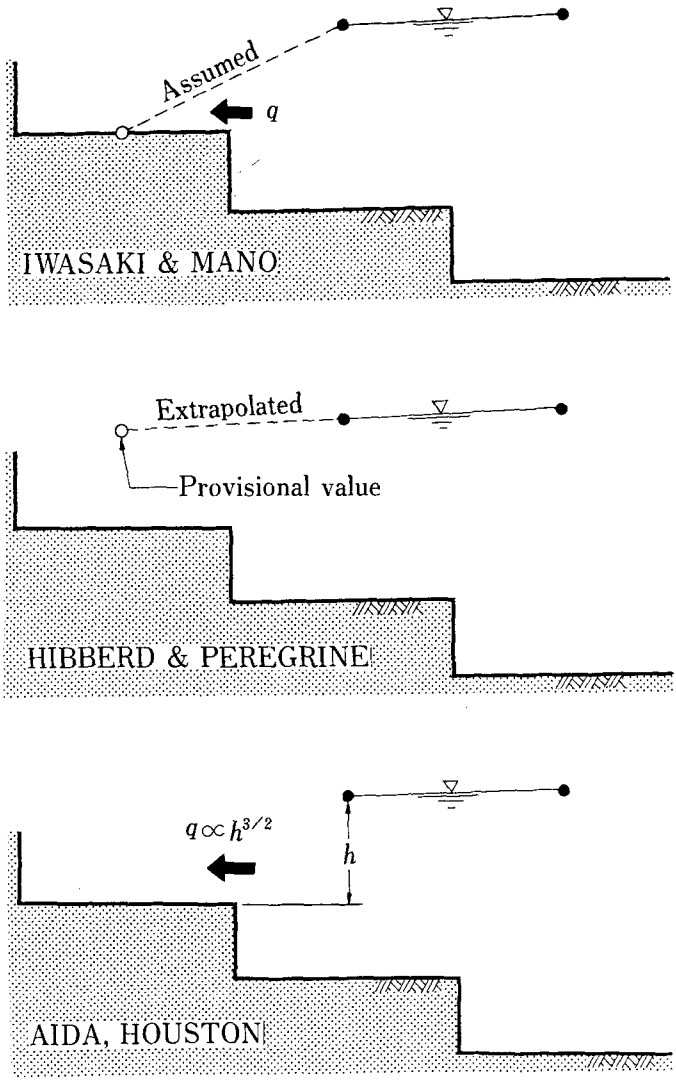

Fig. 10. Approximated moving boundary conditions.

There are several approximate moving boundary conditions. In the leap-frog scheme, grid points are alternatively located for velocity and water level. Assume that the water level is already computed at a computation cell. Then, compare the water level with the bottom height of the next landward cell. If the water level is higher than the latter, the water may flow into the landward cell. Figure 10 explains the ways to estimate the inflow velocity or discharge.

Iwasaki and Mano (1979) assume that the line connecting the water level and the bottom height gives the surface slope to the first-order approximation.

Hibberd and Peregrine (1979) give a provisional water level in the dry cell on a linearly extrapolated water surface. Then, the discharge calculated with this provi-

sional water level gives the total amount of water into the dry cell and the water depth in the cell. If necessary, the computation will be repeated with the water level thus modified.

Aida (1977) and Houston and Butler (1979) evaluate the discharge into the dry cell with broad-crested weir formulas in which the water depth above the bottom of the dry cell is substituted.

These approximations are convenient to handle but introduce numerical errors (Goto and Shuto, 1983a). The run-up height computed with the Iwasaki–Mano method agrees with the theoretical solution with a 5% range of error if the following condition is satisfied

$$\Delta x/\alpha g T^2 < 4 \times 10^{-4}. \tag{7}$$

With the Aida method, the condition is given by

$$\Delta x/\alpha g T^2 < 10^{-3}, \tag{8}$$

in which α is the angle of slope, g is the gravitational acceleration, Δx is the spatial grid length, and T is the wave period.

In closing this section, a comment should be made on the widely-believed opinion that there is no difference between linear and shallow-water theories as far as the maximum run-up height is concerned. In the case of one-dimensional problems, the maximum run-ups are the same even though the two theories give different wave profiles. On the other hand, in a practical problem in which the land has a two-dimensional complicated topography, the lateral flow is induced and affected much by the difference in wave profile; this nonlinearity becomes important.

4.4. *Effect of Large Obstacles*

There are three methods to include the effects of building into tsunami simulation. The simple method in a hindcasting is to allot a large friction coefficient f, which ranges from 0.2 to 1, to the residential areas. This method is, however, not applicable to a forecasting, because an appropriate value of the friction coefficient is determined only after comparisons of the computed inundated area with the recorded. A more reasonable method which can be used in a forecasting is to determine an equivalent friction coefficient by summing up the drag of individual buildings (Goto and Shuto, 1983b). The best way is to use very fine grids in the city area. If the grids are less than 5 m wide, most of the large buildings can be expressed as impermeable boundaries. This inevitably increases the number of grid points. Fine grids also introduce the question of whether or not a map used in discretization is accurate enough for this detailed computation.

In the neighborhood of a large obstacle covered by fine grids, the water flow can be numerically simulated. However, this leaves the question of whether the computed result is reliable. Figure 11 shows an example. Uda *et al.* (1988a) computed a tsunami that overflowed a model sand dune. They compared the results with the

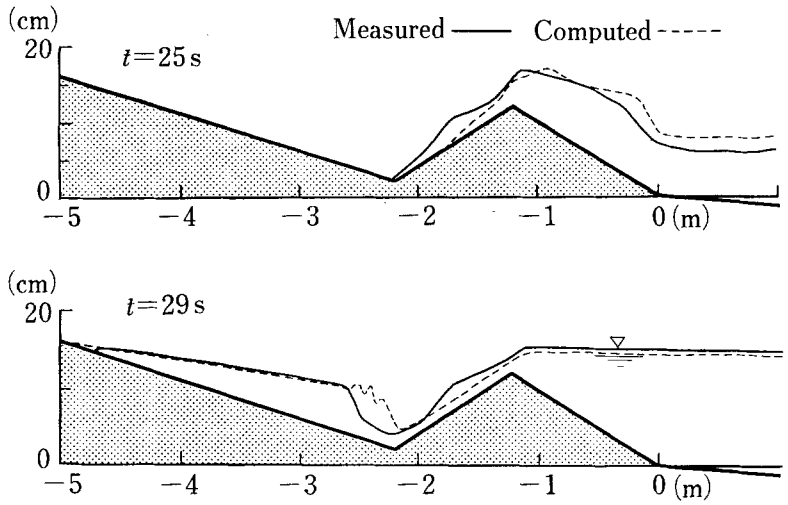

Fig. 11. Computed tsunami profiles overflowing a dune compared with experiments.

measured data in hydraulic experiment. Agreement was poor just behind the dune where the water flow varied from supercritical to subcritical flows through a jump. Then, agreement recovered further behind the dune.

5. Topics for Future Study

5.1. *Edge Bore*

After entering the North Akita coast 55 km long, the 1983 Nihonkai-Chubu earthquake tsunami was trapped along the slightly curved coast of a gentle sandy beach. In photos taken from a coastal hill, it was shown that edge bores hit the coast again and again. Hydraulic experiments carried out in the Public Works Research Institute (Uda *et al.*, 1988b) revealed several interesting phenomena. An edge bore propagates sometimes following the ordinary refraction law and sometimes neglecting the topography. A small difference in the boundary condition might introduce a big difference in wave profile, thus suggesting also a big difference in wave force. No theory and no simulation method are available now.

5.2. *Spread of the Floating Materials*

In the coastal areas, large quantities of oils and timbers are often stored and small fishing boats are often moored in the vicinity of harbors. The presence of these materials increases the danger to the surrounding areas if transported by a tsunami. In 1964, three towns in Alaska were heavily damaged by fires due to oil spills spread by the tsunami. On the occasions of huge tsunamis in the past, timbers, boats, and debris of broken houses changed into formidable destructive forces.

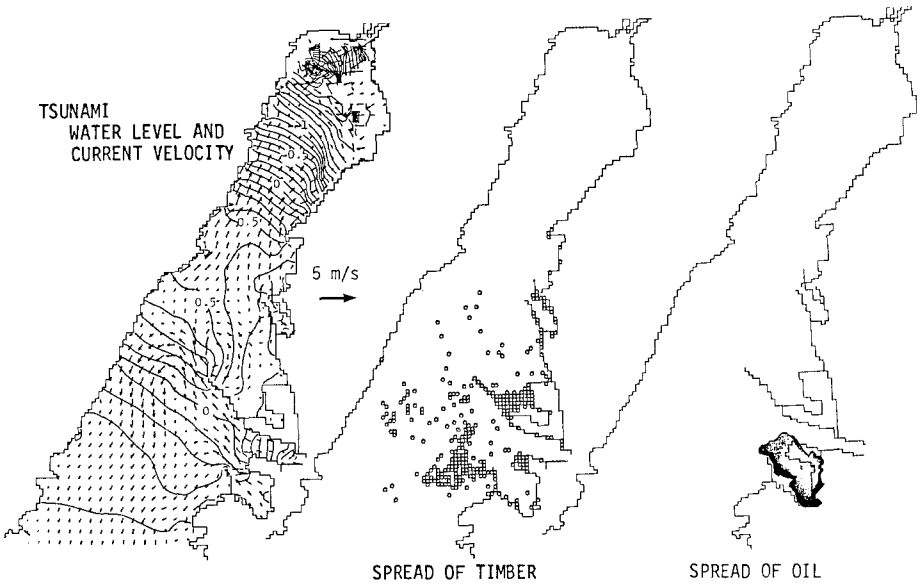

Fig. 12. Spread of oil and timbers due to a tsunami.

Goto developed numerical methods to estimate the spread of oil (1985) and timbers (1983). Figure 12 shows an example. However, these methods have not yet been checked with experimental or measured data.

Although the impact of timbers needs an urgent study for practical design, there is only one paper (Matsutomi, 1989) on this problem.

5.3. *Computer Graphics*

A tsunami numerical simulation creates huge quantities of information, only a few of which are used at present. They are the maximum run-up along the coast, the inundation area, the time history of water level at several selected points, velocity vectors and water level contours at several time intervals, and so on. If a computer-graphic-aided video animation is introduced, the whole computed results would be efficiently used and would reveal the detailed dynamic movement of the tsunami from several viewpoints. The video animation may replace the hydraulic experiment on a large scale to some extent, if we keep in mind that the motion in the animation is limited by the theory used in the simulation.

6. Concluding Remarks

The numerical simulation is now used as a powerful means in the planning of tsunami defense works. A hindcasting can give the maximum run-up height and the corresponding flooded area within a 15% error. This does not, however, mean that tsunami waves are always correctly reproduced. From the generation to the final

effect, there is no exact way to calibrate the computed wave profiles, because of the shortage and poor resolution ability of tsunami gauges. The most urgent and necessary problem in developing simulation techniques is not the simulation itself but revealing the truth of tsunamis through observation networks of high accuracy. Tsunami gauges in deep sea are not enough in number to catch tsunamis in infancy, which will provide a way to check the present method of determination of the initial tsunami profile. Tide gauges near land should be improved to overcome their poor temporal resolution and possible scale-out in case of a huge tsunami, although there is a way to improve its hydraulic attenuation characteristics.

As for currents and wave forces that are important from the viewpoint of structure design, comparisons of the computed results with hydraulic experiments of large scale may be the only possible way of calibration.

If a forecasting is required, there are several problems to be solved in the near future.

References

Aida, I.: 1977, Numerical experiments for inundation of tsunamis, Susaki and Usa, in the Kochi Prefecture, *Bull. Earthq. Res. Inst.* **52**, 441–160 (in Japanese).

Aida, I.: 1978, Reliability of a tsunami source model derived from fault parameters, *J. Phys. Earth* **26**, 57–73.

Aida, I.: 1984a, A source model of the tsunami accompanying the 1983 Nihonkai-Chubu earthquake, *Bull. Earthq. Res. Inst.* **59**, 235–265 (in Japanese).

Aida, I.: 1984b, Source models of the 1983 Nihonkai-Chubu earthquake tsunami, *Proc. Symp. Nihonkai-Chubu Earthquake Tsunami*, JSCE, pp. 9–21 (in Japanese).

Aida, I. and Hatori, T.: 1983, Numerical simulation of tsunami inundation in Yuasa and Hirokawa towns, Wakayama Prefecture in southwestern Japan, *Bull. Earthq. Res. Inst.* **58**, 667–681 (in Japanese).

Goto, C.: 1983, Numerical simulation of spread of floating timbers, *Proc. 30th Conf. Coastal Eng.*, JSCE, pp. 594–597 (in Japanese).

Goto, C.: 1984, Equations of nonlinear dispersive long waves for a large Ursell number, *Proc. JSCE* **351/II-2**, 193–201 (in Japanese).

Goto, C.: 1985, A simulation model of oil spread due to tsunamis, *Proc. JSCE* **357/II-3**, 217–223 (in Japanese).

Goto, C. and Shuto, N.: 1983a, Numerical simulation of tsunami propagations and run-up, in K. Iida and T. Iwasaki (eds.), *Tsunamis: Their Science and Engineering*, Terra Science Pub. Co., Tokyo/Reidel, Dordrecht, pp. 439–451.

Goto, C. and Shuto, N.: 1983b, Effects of large obstacles on tsunami inundations, in K. Iida and T. Iwasaki (eds.), *Tsunamis: Their Science and Engineering*, Terra Science Pub. Co., Tokyo/Reidel, Dordrecht, pp. 551–525.

Hasegawa, K.: 1986, Numerical simulations to substantiate past tsunamis for the planning of prevention works, Doctoral dissertation, Kyoto Univ. (in Japanese).

Hibberd, S. and Peregrine, D. H.: 1979, Surf and run-up on a beach: a uniform bore, *J. Fluid Mech.* **95**, 323–345.

Houston, J. R. and Butler, H. L.: 1979, A numerical model for tsunami inundation, WES Tech. Rep. HL-79-2.

Imamura, F.: 1989, Possibility of tsunami numerical forecasting, Doctoral dissertation, Tohoku Univ. (in Japanese).

Iwasaki, T. and Mano, A.: 1979, Two-dimensional numerical simulation of tsunami run-ups in the Eulerian description, *Proc. 26th Conf. Coastal Eng.*, JSCE, pp. 70–74 (in Japanese).

Kajiura, K.: 1963, The leading wave of a tsunami, *Bull. Earthq. Res. Inst.* **41**, 535–571.

Mansinha, L. and Smylie, D. E.: 1971, The displacement of the earthquake fault model, *Bull. Seismol. Soc. Amer.* **61**, 1433–1400.

Matsutomi, H.: 1989, Impact of breaking bore accompanying floating timbers, *Proc. Coastal Eng*, JSCE, 36, pp. 574–578 (in Japanese).

Peregrine, D. H.: 1967, Long waves on a beach, *J. Fluid Mech.* **27**, 815–827.

Plafker, G.: 1965, Tectonic deformation associated with the 1964 Alaska earthquake, *Science* **148**, 1675–1687.

Satake, K.: 1985, The mechanism of the 1983 Japan Sea earthquake as inferred from long period surface waves and tsunamis, *Phys. Earth Planet. Interiors* **37**, 249–260.

Satake, K. *et al.*: 1988, Tide gauge response to tsunamis: Measurements at 40 tide gauge stations in Japan, *J. Marine Res.* **46**, 557–571.

Shuto, N. and Goto, C.: 1978, Numerical simulation of tsunami run-up, *Coastal Engineering in Japan* **21**, 13–20.

Shuto, N. *et al.*: 1986, A study of numerical techniques on the tsunami propagation and run-up, *Sci. Tsunami Hazard* **4**, 111–124.

Shuto, N. *et al.*: 1987, Numerical simulation of tsunami propagations and run-ups on historical tsunamis—Summary, *Proc. Interational Tsunami Sym.*, NOAA, 184–187.

Takagi, A. *et al.*: 1984, Earthquake activities before and after the main shock, in K. Noritomi (ed.), General report on the disasters caused by the 1983 Nihonkai-Chubu earthquake, Rep. No. 58022002, supported by the Ministry of Education, Culture and Science, pp. 24–30 (in Japanese).

Takeda, H.: 1984, Numerical simulation of run-up by variable transformation, *J. Oceanogr. Soc. Japan* **40**, 271–278.

Tanaka, K. *et al.*: 1984, Characteristics of the Nihonkai-Chubu Earthquake, in K. Noritomi (ed.), General Rep. on the Disasters Caused by the 1983 Nihonkai-Chubu Earthquake, Rep. No. 58022002, supported by the Ministry of Education, Culture and Science, pp. 39–45 (in Japanese).

Uda, T. *et al.*: 1988a, Numerical simulation and experiment on tsunami run-up, *Coastal Eng. in Japan*, JSCE **31**, 87–104.

Uda, T. *et al.*: 1988b, Two-dimensional deformation of nonlinear long waves on a beach, Rep. Public Works Res. Inst., Minsistry of Construction, Japan, No. 2627 (in Japanese).